Tunisian hypersaline sediments to set up suitable halotolerant microbial bioanodes for electrostimulated biodegradation of thiabendazole

Nesrine Saidi, Benjamin Erable, Sirine Saadaoui, Rim Driouech, Amira Zaouak, Haikel Jelassi, Mohamed Neifar, Ahmed Slaheddine Masmoudi, Ameur Cherif, Habib Chouchane

frontiers | Frontiers in Energy Research

TYPE Original Research
PUBLISHED 01 September 2022
DOI 10.3389/fenrg.2022.981802

OPEN ACCESS

EDITED BY
Siddharth Gadkari,
University of Surrey, United Kingdom

REVIEWED BY
Sovik Das,
Indian Institutes of Technology (IIT), India
Indrasis Das,
Central Leather Research Institute (CSIR), India

*CORRESPONDENCE
Benjamin Erable,
benjamin.erable@ensiacet.fr
Habib Chouchane,
habib.chouchane@isbst.uma.tn

SPECIALTY SECTION
This article was submitted to Bioenergy and Biofuels, a section of the journal Frontiers in Energy Research

RECEIVED 29 June 2022
ACCEPTED 05 August 2022
PUBLISHED 01 September 2022

CITATION
Saidi N, Erable B, Saadaoui S, Driouech R, Zaouak A, Jelassi H, Neifar M, Masmoudi AS, Cherif A and Chouchane H (2022), Tunisian hypersaline sediments to set up suitable halotolerant microbial bioanodes for electrostimulated biodegradation of thiabendazole.
Front. Energy Res. 10:981802.
doi: 10.3389/fenrg.2022.981802

Tunisian hypersaline sediments to set up suitable halotolerant microbial bioanodes for electrostimulated biodegradation of thiabendazole

Nesrine Saidi[1], Benjamin Erable[2]*, Sirine Saadaoui[1,2], Rim Driouech[1], Amira Zaouak[3], Haikel Jelassi[3], Mohamed Neifar[1], Ahmed Slaheddine Masmoudi[1], Ameur Cherif[1] and Habib Chouchane[1]*

[1]ISBST, BVBGR-LR11ES31, Biotechpole Sidi Thabet, University of Manouba, Ariana, Tunisia, [2]Laboratoire de Génie Chimique, CNRS, INPT, UPS, Université de Toulouse, Toulouse, France, [3]Laboratory on Energy and Matter for Nuclear Sciences Development, Tunisia. National Center for Nuclear Sciences and Technologies, Sidi Thabet Technopark 2020, Ariana, Tunisia

This study investigated for the first time the performance of microbial halotolerant bioanodes designed from two Tunisian Hypersaline Sediments (THS) for simultaneous electrostimulated biodegradation of synthetic fruit packaging wastewater containing thiabendazole (TBZ), and recovery of an anodic current signal. Halotolerant bioanodes formation has been conducted on 6 cm^2 carbon felt electrodes polarized at −0.1V*vs* Saturated Calomel Electrode (SCE), inoculated with 80% (v:v) of synthetic wastewater containing 50 ppm of irradiated or not irradiated TBZ and 20% (v:v) of THS for a period of 7 days. Microbial bioanodes, and the corresponding anolytes, i.e., synthetic wastewater, were studied comparatively by electrochemical, microscopic, spectroscopic, molecular and microbial ecology tools. Despite the low maximum current densities recorded in the 50 ppm TBZ runs (3.66 mA/m^2), more than 80% of the TBZ was degraded when non-irradiated TBZ (nTBZ) was used as the sole carbon energy by the microorganisms. Nevertheless, the degradation in the presence of irradiated TBZ (iTBZ) was greatly reduced by increasing the irradiation dose with maximum current density of 0.95 mA/m^2 and a degradation rate less than 50% of iTBZ. In addition, chemical changes were observed in TBZ as a result of gamma irradiation and bioelectrochemical degradation. FT-IR and UV-Vis techniques confirmed the degradation of TBZ structural bonds producing novel functional groups. Culture-dependent approach and 16S ribosomal RNA sequencing demonstrated that bacterial community of halotolerant bioanodes formed with nTBZ were dominated by *Proteobacteria* (75%) and *Firmicutes* (25%). At species level, enrichment of *Halomonas smyrnensis*, *Halomonas halophila*, *Halomonas salina*, *Halomonasor ganivorans* and *Halomonas koreensis* on carbon felt electrodes were correlated with maximal current production and nTBZ degradation. As a result, THS halotolerant bacteria, and specifically those from Chott El Djerid (CJ) site certainly have well established application for

the electrostimulated microbial biodegradation of fungicide in the real fruit and vegetable processing industries.

KEYWORDS

halotolerant microbial bioanodes, tunisian hypersaline sediment, fruit packaging wastewater, microbial electrostimulated degradation, fungicide pollutant, gamma irradiation

1 Introduction

Thiabendazole (TBZ) is one of the most used chemicals as a postharvest fungicide in fruit packaging industries. These industries consume large quantities of water and generate large volumes of fruits packaging wastewater (FPWW) containing high concentration of TBZ ranging from 0.25–0.45 g/L or banana, avocado and mango to 2 and 30 g/L for citrus and potato seeds, respectively (European Commission, 2013). The extensive use of TBZ has led to its frequent detection in the surface and groundwater (Castillo et al., 2000; Masiá et al., 2013; Perruchon et al., 2017). This has raised serious environmental concerns mainly related to TBZ high half-life in soil which is between 833 and 1,444 days (Papadopoulou, et al., 2018). As reported by Qian et al. (2008), TBZ is considered a persistent environmental contaminant and potentially toxic to the aquatic environment. Papadopoulou et al. (2018) demonstrated that the toxicity of TBZ determined by the median effective concentration (EC50) in salmonid species (*Oncorhynchus mykiss*) is 0.55 10^{-3} g/L. According to the European Commission (European Commission, 2001), wastewater effluents containing high loads of TBZ are considered hazardous and they must be treated on site before their final release to the environment to avoid deleterious effects on the ecological and chemical integrity of natural resources.

Consequently, several wastewater treatment technologies have been designed and applied at laboratory scale first, and then adapted at an operating industrial scale to deal with this issue. Among them, the most advanced technologies are activated carbon filtration, SiO_2-assisted photocatalysis, Fenton oxidation neither alone or in combination with membrane biological processes (Portillo et al., 2004; Peréz et al., 2014; Carra et al., 2015; Jiménez et al., 2015). Despite their considerable performances, these methods have not been commercialized due to 1) their high cost of large-scale implementation in fruit packaging plants, 2) problems associated with the generation of intermediate metabolites of unknown toxicity, and 3) the fact that their efficiencies have been demonstrated at low TBZ concentrations that are below TBZ levels in wastewater. More information regarding the relative advantages and disadvantages of each technology are discussed in Priyadarshini et al. (2022). This lack of available options has forced industries in the fruit and vegetable packing sector to discharge their effluent either in municipal treatment plants or at adjacent field sites (Papadopoulou et al., 2018). Biological methods are qualified as the most sustainable technologies for several wastewater treatment containing recalcitrant pollutants (Chandrakant et al., 2016; Jiang et al., 2018). Nevertheless, they are not able to guarantee the achievement of required results of treatment of FPWW, as some of fungicide molecules such as TBZ are hazardous and/or recalcitrant to microorganism driven degradation. The most convenient method must enable the degradation of resistant compounds, cost-effective, and produce a safe and eco-friendly effluent. There is therefore a pressing environmental and economic need to design and develop a treatment technology that addresses these major challenges.

Tough, resilient, and exoelectrogenic microorganisms from extreme environments (Cherif et al., 2017; Ben Abdallah et al., 2018; Askri et al., 2019) used as inoculums in microbial electrochemical systems could fulfill the double function of degrading the TBZ and recovering the energy resulting from its oxidation, or at least directly follow its fate in solution by measuring the specific current of its oxidation. Previous studies have demonstrated that exoelectrogenic populations have favorably contributed to the treatment of recalcitrant pollutants, such as azo dyes, heavy metals, and petroleum hydrocarbons (Grattieri and Minteer, 2018; Vijay et al., 2018; Elabed et al., 2019; Askri et al., 2020). Askri et al. (2020) demonstrated the high performance of microbial bioanodes enriched from bacterial communities of Tunisian extreme environment saline sediments and real textile wastewater for degrading dyes at 91 ± 3% and recovering electric current streams up to 12.5 ± 0.2 A/m^2. On the basis of these observations, the objective of this study was to demonstrate the feasibility of designing new halotolerant microbial bioanodes (HMB) capable of degrading a recalcitrant fungicide, i.e. TBZ. The outstanding originality of this HMB design is based on the exploitation of the natural bacterial community of two types of hypersaline sediments from the Tunisian desert. In addition, the contribution of gamma irradiation of TBZ at increasing dose as a pre-treatment for TBZ degradation was also investigated.

Once the potential degradation of TBZ as a result of irradiation was quantified, the bioelectrochemical degradation of irradiated or unirradiated TBZ and the corresponding current generation by HMBs was demonstrated and quantified by coupling electrochemical measurements of the current exchanged by the bacteria and monitoring of specific TBZ signatures by Fourier-transform infrared spectroscopy (FTIR) and combined UV-Visible analysis. Finally, additional

microscopic and microbiological post-operation investigations allowed us to understand which communities had settled on the HMBs.

2 Materials and methods

2.1 Collection of hypersaline sediments samples

Hypersaline sediments used as a source of halophilic microorganisms were collected from two extreme salt lakes, Chott El Djerid (CJ) and Sebkhet El Melah (SM), located in the south of Tunisia (N:33°57.272' E: 008°24.393′ and N: 33°23.705′ E: 010°54.878, respectively) during the wet season (February). Samples were secured in sterile bags and stored at +4°C until utilization.

2.2 Composition of the synthetic fruit packaging wastewater

All experiments were carried out in minimal salt medium supplemented with TBZ as the sole carbon source. The detailed composition of the minimal salt medium was (per liter): 150 g NaCl, 0.5 g K_2HPO_4, 1 g NH_4Cl_2, 2 g $MgCl_2$, 0.1 g $CaCl_2$.

50 ppm of TBZ was added of either native or irradiated. An analytical standard of TBZ (≥99% purity, Sigma-Aldrich) was used for analytical purposes analyses and culture experiments. pH and temperature were adjusted at 7.2 and 38°C, respectively.

2.3 Gamma irradiation methodology

Aqueous solutions of TBZ were irradiated by a Cobalt 60 γ-source. Irradiation processes were performed in the National Centre of Nuclear Sciences and Technologies (CNSTN) at Sidi-Thabet, Tunisia. For an accurate control of the irradiation time, a specific determination of the dose rate is necessary. Dose rates of 26.31 and 6.81 Gy/min were determined with Red Perspex dosimeters (M'Garrech et al., 2012). The doses applied were 1, 2, and 4 kGy. The method of dose rate measurement is described in Ounalli et al. (2017). It is important to mention that when gamma rays interact with water, unstable and stable oxidizing and reducing species are formed and will act as modifiers of the TBZ structure.

2.4 Reactors setup and electrochemical protocols

Single-chamber 750 ml glass reactors equipped with a three-electrode system were used for microbial anodes formation. A carbon felt (6 × 1 × 1 cm^3, Mersen) was used as a working electrode (WE). A platinum grid (Heraeus) was used as the auxiliary electrode (AE), and a saturated calomel reference electrode (+0.24 V/SHE, Origalys) was located between the WE and the AE. The three electrodes were connected to a multichannel Potentiostat/Galvanostat (OGF 500, Origalys) managed by the OrigaMaster five software (Figure 1). Constant polarization at −0.10 V vs. SCE was applied on the WE. Chronoamperometric maximum current densities (CA) of microbial bioanodes were determined as indicated in our previous studies (Askri et al., 2019–2020).

2.5 Global and detailed biofilm architecture

The global 3D structure of biofilms and the distribution of microorganisms on the carbon fibers of anodes were investigated using epifluorescence microscopy. At the end of the 7 days of microbial anodes formation, a first part of the WE covered by THS enriched biofilms was stained immediately with acridine orange 0.01% (A6014 Sigma) for 10 min then washed and dried at room temperature for 24 h. Biofilms architecture was observed with a Carl Zeiss Axio ImagerM2 microscope motorized in Z and equipped with a UV light source (HBO 200) and a Zeiss 09 filter (HP450-490 exciter, FT-10 reflector, LP520 barrier filter). Image acquisition is performed with a Zeiss digital monochrome camera (AxioCammm RM). With the help of the Zen software, the images are processed to obtain projections from the acquisition of image stacks scanning several tens of µm in biofilm thickness.

2.6 Analysis of TBZ degradation

2.6.1 COD measurement

The chemical oxygen demand (COD) removal rate (%) corresponds to the percentage of the total organic matter eliminated in the synthetic FVPWW containing irradiated or not irradiated TBZ. Samples were recuperated from anolytes of each reactor and the COD was measured by potassium dichromate method using LCK 514 (100–2000 mg O_2/L) after a 1/6 dilution. Chloride elimination kit LCW925 (Hach Lange) was used to remove chloride ions in different samples. The COD removal rate (COD_{rr}) was measured as shown in the following formula:

$$COD_{rr} = 1 - \frac{CODeffluent}{CODinfluent} \times 100 \quad (1)$$

2.6.2 UV-visible analysis

UV-spectral analysis of synthetic filtered FVPWW (i.e., without cells and particles) was monitored in order to determine the TBZ concentration decrease after irradiation

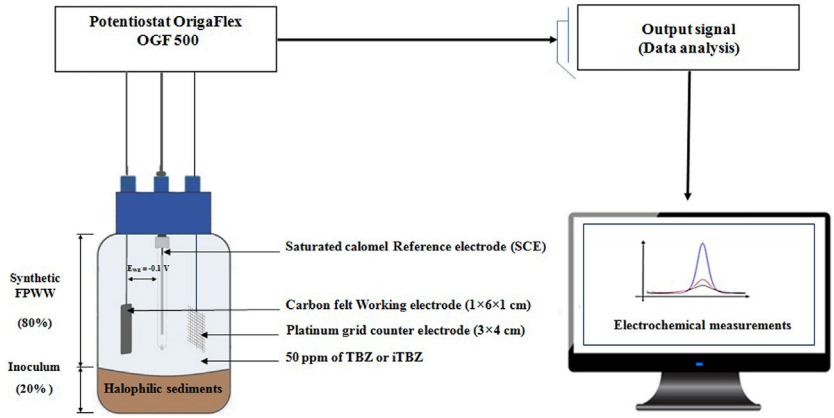

FIGURE 1
Schematic representation of microbial electrolysis cell (MEC) and bioelectrochemical protocol.

and bioelectrochemical treatments. 50 ppm of irradiated and unirradiated TBZ solutions were used as references. Changes in their absorption spectrum were carried out using UNICO 2080 spectrophotometer in the ultraviolet region.

2.6.3 FTIR analysis

The possible changes in functional groups of TBZ after irradiation treatment and bioelectrochemical degradation were detected using Fourier Transform Infrared Spectroscopy under ambient conditions using the transmission mode (%T). The measurements were carried out in the range 4,000–400 cm^{-1} using an FTIR apparatus (Perkin Elmer model) with a speed of 16 scans. TBZ powder form (≥99% purity) was used as control. Samples were filtered using a 0.45 μm syringe filter to remove particles.

2.7 Microbial analysis

After 7 days of operation, both the anodic biofilm and the bacterial pool present in the electrolyte were collected from the reactor in which the bioelectrochemical degradation of nTBZ occurred by using CJ sediments as inoculum (CJ nTBZ experiment). Culture depended approach was carried on to phylogenetically characterize the existing community in the sediments leading to TBZ degradation and current production. For molecular identification, portion of the bioanode (about 2 cm) and 5 ml of electrolyte were separately added to sterile test tube containing physiological solution (0.9% NaCl). After a serial dilution (10^{-1} to 10^{-7}), in the culture medium described above supplemented with 15% agar, successive subcultures were performed at 38°C until isolation of pure strains. Genomic DNA from pure strains was extracted by Organic (Phenol–Chloroform) method (Li et al., 2007). DNA quality and quantity were measured by a Thermo Scientific NanoDrop™ ND-2000 Spectrophotometer (Thermo Fisher Scientific, Waltham, MA, United States). PCR reactions and sequencing were performed based on 16S rRNA gene using universal bacteria primers S-D-Bact-0008-a-S-20/ S-D-Bact1495-a-A-20 (Ettoumi et al., 2013). 16S rDNA sequencing was carried out in the research and technology transfer support unit at the BorjCedria Biotechnology Center. DNA sequences were edited using BioEdit software. The resulting 16S rDNA sequences were used via EzBioCloud (Yoon et al., 2017) to determine the taxonomy of the strains. The phylogenetic dendrograms was constructed using the phylogeny. fr website.

3 Results and discussion

3.1 Measurement of the exo-electric current transferred to the carbon-felt electrode and the degradation of native TBZ (nTBZ) and pre-irradiated TBZ (iTBZ)

Two distinct types of extreme Tunisian hypersaline sediments (THS) were compared as a source of halophilic microorganisms for 1) forming anodic biofilms on carbon-felt electrodes, and 2) biodegrading native TBZ (nTBZ) and TBZ pre-irradiated (iTBZ) with increasing gamma irradiation doses. Both forms of TBZ were provided as the exclusive substrate, it is the only possible source of energy and organic carbon for the microorganisms. Overall, eight electrochemical experiments were performed with a synthetic FPWW. The performance of the THS for current production and TBZ degradation was evaluated using nTBZ and iTBZ separately. Current densities, cumulated charges, Coulombic efficiencies and COD removals determined from different

TABLE 1 Comparative table of bioelectrochemichal approaches (voltage, power density, Coulombic efficiency, removal efficiency) for different recalcitrant pollutants remediation. Chott El Djerid (CJ) and Sebkhet El Melah (SM) sediments performances were measured under identical conditions for both bioelectrochemical and biological experiments.

	Bioelectrochemical experiments									Biological experiments		
Recalcitrant remediated	**Type of inoculum**	**Type of BES**	**Anode type/ applied voltage**	**Max current density (mA/m^2)**	**Max power density (mW/m^2)**	**Cumulated charge on 7 days (coulomb)**	**CE (%)**	**Initial COD (mg O_2/L)**	**Final COD (mg O_2/L)**	**Removal efficiency (%)**	**COD removal rate (%)**	**References**
Ibuprofen (IBU)	Domestic wastewater	Two chamber MFC	Graphite fiber brushe/+0.5 V	nd[a]	nd	nd	nd	nd	nd	64.28	nd	Wang et al., (2022)
Total petroleum hydrocarbons (TPHs)	Peat moss and soil	Soil-based MFC	Titanium wire/ +0.44 V	nd	276	nd	nd	nd	nd	49.38	nd	Mohanakrishna et al., (2019)
Dye	dye waste water	Single chamber (MFC)	Anode brush with a core of titanium wires tips of carbon fibers	nd	515	nd	56	nd	nd	85	nd	Karuppiah et al., (2018)
nTBZ	CJ Sediments	Single chamber Microbial electrolysis cell (MEC)	Carbon felt/-0.1 V	3.66	nd	8.67	0.2	750	147	80.45	42.83	This study
iTBZ-1kGy				0.94	nd	49.1	0.02	2040	1122	45.00	35.87	
iTBZ-2kGy				0.83	nd	3.85	0.06	2000	1096	45.23	42.86	
iTBZ-4kGy				1.40	nd	4.07	0.08	915	221	75.85	74.86	
nTBZ	SM Sediments			0.95	nd	0.94	0.13	644	547	15.06	nd	
iTBZ-1kGy				1.47	nd	2.25	0.06	1925	1482	23.01	nd	
iTBZ-2kGy				0.68	nd	0.50	0.03	1895	1687	10.97	nd	
iTBZ-4kGy				0.11	nd	0.19	nd	810	nd	nd	nd	

[a]Not determined.

10.3389/fenrg.2022.981802

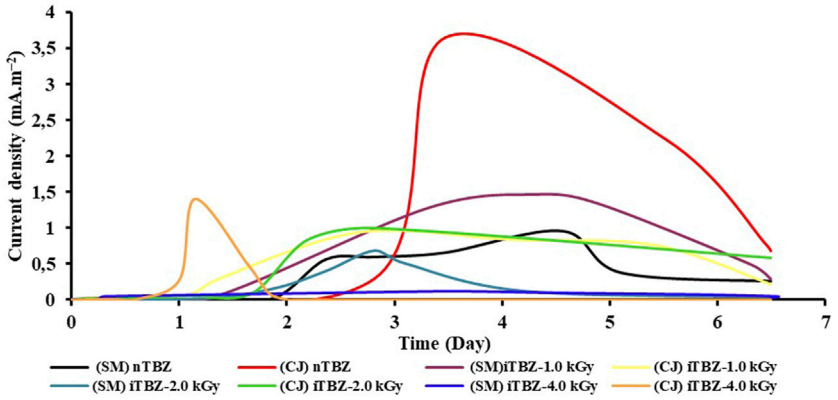

FIGURE 2
Evolution of the current density (mA/m^2) versus time (day) using native TBZ (nTBZ) or pre-irradiated TBZ (iTBZ) as electron donor on a carbon felt electrode inoculated with Sebkhet El Melah sediment (SM) or Chott El-Djerid sediment (CJ).

experiments for both sources of microorganisms are summarized in Table 1. The detail of the eight chronoamperometric curves is shown in Figure 2. A control experiment without the presence of electrodes was also conducted with sediments from CJ. The SM sediment shows lower performance compared to the CJ sediment particularly in terms of current densities and Coulombic efficiencies. A decrease in current densities exceeding 70 and 90% is noted for nTBZ and iTBZ-4kGy, respectively (Table 1). As the experiments were performed under the same conditions, microorganisms hosting the SM sediments could be unable to degrade TBZ even in its irradiated form. As demonstrated in Table 1, CJ sediment supported higher COD removal (>80%) than SM sediments. The removal efficiency of nTBZ (>80%) was comparable to that of azo-dye (85%) (Karuppiah et al., 2018) and better than those of petroleum hydrocarbons (49.38%) (Mohanakrishna et al., 2019) and Ibuprofen (64.28%) (Wang et al., 2022).

Table 1 showed that initial COD of iTBZ may increase with elevated irradiation doses (1 and 2 kGy). In contrast, a declining trend in COD removal rate efficiency, accompanied by a decrease in current generation, was observed. Contrary to what was expected irradiation pretreatment of TBZ had prominent negative effect on both the COD removal and the current generation. In fact, with CJ as inoculum, the 7 days COD removal rate of 50 ppm nTBZ was 1.78 and 1.77 times of those for iTBZ-1.0 kGy and iTBZ-2.0 kGy, respectively. Similarly, maximum current density of nTBZ was 4.21 and 4.77 times of those monitored for iTBZ-1.0 kGy and iTBZ-2.0 kGy, respectively.

In general, the evolution of the current density as a function of time (Figure 2) is well consistent with what is known about the formation of an anodic biofilm on carbon-felt electrodes. Thus, taking the experiments with nTBZ as an illustration evolution of the electrochemical activity is analogous to the successive formation and growth phases of electroactive bacterial biofilms on the working electrode (Baranitharan et al., 2015). Latent phase, at zero current, during this period, the bacteria adapted to the sessile lifestyle by progressive colonization at the surface of the anode using nTBZ as electron donors. Followed by a low anodic current that slowly increased to attend their maximum explained by the nTBZ or iTBZ oxidation. The production of current continued to increase to reach maximum current densities at the end of the experiment of 0.95 and 3.66 mA/m^2, for SM and CJ inoculums, respectively. Previous studies using CJ as inoculum, with lactate (5 g/L) or real textile wastewater as energy sources, have demonstrated the ability to design electroactive bioanodes with current production of 6.98 ± 0.06 and 12.50 ± 0.20 A/m^2, respectively. Additionally, the COD removal rate was 91 ± 3% when real textile wastewater containing azo-dyes was used as energy substrate (Askri et al., 2019; Askri et al., 2020). In this study, a comparable COD removal was obtained (>80%) in particular with nTBZ. However, the current production remains very low (0.003 A/m^2).

The increase of the irradiation doses on the iTBZ resulted in a very important decrease in current generation in the case of both sources of inoculum (Figure 2 and Table 1). And even an almost zero current production is recorded for the pre-treated iTBZ-4.0 kGy. However, the COD removal rate is 75.85%. It is both very similar to that obtained with nTBZ in the bioelectrochemical experiments and to that resulting from the biological degradation experiments of iTBZ-4.0 kGy without electrode. In all the cases studied, the gamma irradiation did not improve the anodic current resulting from the oxidation of iTBZ. LC-MS analysis of the irradiation degradation products and the evaluation of their toxicity towards microorganisms could clarify the observed effect of the gamma irradiation of TBZ.

In fact, the monitoring of nTBZ and iTBZ biodegradation by measuring the optical density at specific wavelengths demonstrated a degradation rate less than 50% in different

synthetic FVPWW containing iTBZ as substrate. However, the degradation rate was >80% when nTBZ was used with CJ as inoculum. Despite this high degradation rate of nTBZ, the current density produced remains really weak. This could be explained by the fact that several bacteria in the synthetic FVPWW non-anode adherent microorganisms and called "planktonic" consume almost all of the nTBZ in the synthetic FVPWW without participating in the current production. Consequently, the competition for oxidizing nTBZ between electroactive and non-electroactive bacterial species results in a low current density in chronoamperometric experiments. It is particularly important to note that microbial electrochemical processes involving bioremediation of recalcitrant pollutants do not have energy as the main output (Liang et al., 2020). However, weak electrostimulation (ES) could be necessary for enhancing the microbial transformation of nTBZ. Ailijiang et al. (2016) reported that ES (2 mA) is potentially effective for biofilm reactors treating phenol-containing wastewater. More recently Wang et al. (2022), demonstrated that weak ES enhanced the microbial transformation of anti-inflammatory recalcitrant drugs such as ibuprofen and naproxen. The weak ES could influence the growth of cells and metabolic behaviors of microorganisms. In this study, the electrostimulated biodegradation removal rate of nTBZ after 7 days was greater than 80%, which corresponds to an abatement of the concentration of 40 ± 0.5 ppm of nTBZ with CJ as inoculum. In terms of bioremediation these results could be very conclusive compared to those already obtained by Perruchon et al. (2017) using bacterial consortium isolated from wastewater disposal site adjacent to a citrus fruit packaging plant and 20 ppm of TBZ as initial concentration.

Halophilic sediments such as CJ have shown in previous works their efficiency in designing halotolerant bioanode able to degrade azo dyes in textile wastewater with more than 90% of COD removal rate (Askri et al., 2020). Moreover Pugazhendi et al. (2020) reached a COD removal efficiency of up to 89% when used halophilic microorganisms to treat seafood industrial wastewater. Similarly, Feng et al. (2015) reported enhanced removal of recalcitrant p-Fluoronitrobenzene when a MEC was operated at highly saline conditions. In view of the findings CJ sediment is a promising potential source of tenacious exoelectrogenic halophilic microorganisms for enriching the microbial communities on the anode to degrade nTBZ or iTBZ. Consequently, CJ sediments are the subject of more in-depth investigations in this study.

3.2 Microbial colonization of polarized carbon felt electrodes exposed to nTBZ and iTBZ

It is clear at this stage of understanding that the conversion of TBZ, whether irradiated or not, is not linked to the direct oxidative action of an electroactive biofilm established on the surface of the carbon felt. The recorded current densities, and especially the low Coulombic efficiency calculations (Table 1),

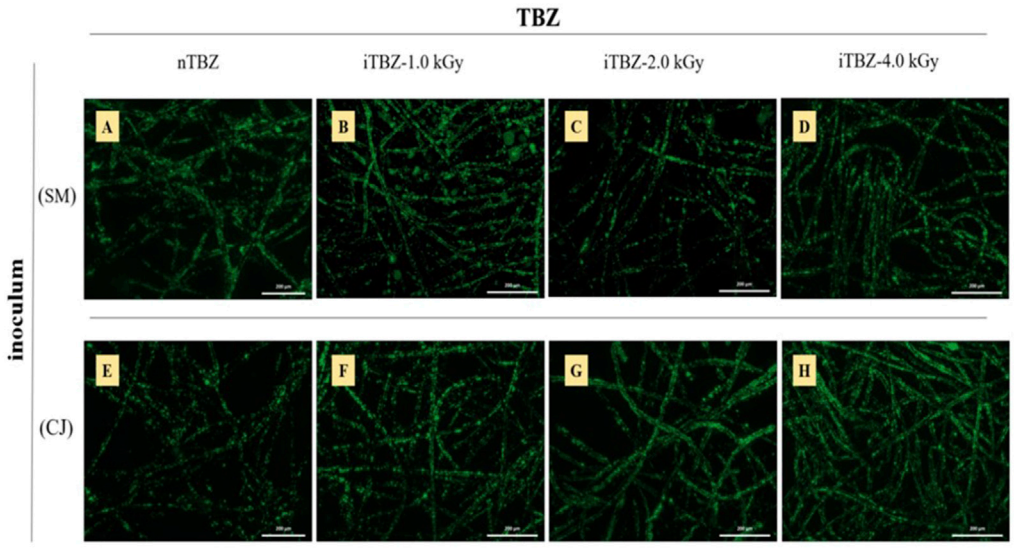

FIGURE 3
Assessment of microbial proliferation on the outer surface of carbon felt electrodes by epifluorescence microscopy imaging. The surface of the carbon felt electrode was stained with acridine orange to localize microbial cells. Bioanodes were formed at different inoculums and with nTBZ or iTBZ **(A)** SM and nTBZ **(B)** SM and iTBZ-1.0 kGy **(C)** SM and iTBZ-2.0kGy **(D)** SM and iTBZ-4.0kGy **(E)** CJ and nTBZ **(F)** CJ and iTBZ-1.0kGy **(G)** CJ and iTBZ-2.0kGy **(H)** CJ and iTBZ-4.0 kGy.

rather suggest an electrostimulation activity that would boost the biodegradation activity of TBZ. This electrostimulation, effective via an electrode polarized at −0.10 V/SCE, clearly allows an increase in the TBZ removal rate of 1% in the least convincing case of iTBZ-4.0 kGy and up to 38% in the most conclusive case of nTBZ removal.

In any case, even if an anodic electroactive biofilm does not seem to play a major role, the external surface of the carbon-felt electrodes was still imaged in search of microorganisms that could be electrostimulated by the presence of the polarized electrode. At the end of the chronoamperometries at -0.10 V/SCE, the carbon felt working electrodes were removed from the reactors containing nTBZ, iTBZ with SM and CJ as inoculums. As a reminder, these electrodes produced maximum current densities of 0.95–3.66 mA/m^2, and TBZ removal rates of 81 to 48.99%. The electrodes have been stained with a fluorescent dye that is selective for nucleic acids, and therefore able to detect any microorganisms on the surface of the carbon fibers of the felt. The external surfaces of the electrodes were imaged by epifluorescence microscopy (Figure 3).

Despite the very low current densities detected, all electrodes appear to host a biofilm of microorganisms. In general, the colonization is mostly centred on the surface of the carbon felt fibers without any real continuous proliferation or interconnection between the carbon fibers. This is already characteristic of saline environments where microorganisms are more likely to form electroactive biofilms strongly sheathing the fibers of conductive materials (Rousseau et al., 2014; Askri et al., 2019). Although in our work the biofilms are not very electroactive, the findings seem to conclude that the structural organization of the biofilms is the same.

In terms of biofilm density on the electrode surface, the two inocula induce different colonization rates in the presence of either more or less irradiated iTBZ. In the case of SM THS, colonization appears to be maximal in the presence of nTBZ or low-irradiated iTBZ (iTBZ-1.0 kGy), then the colonization rate appears to collapse as the TBZ irradiation dose increases. In contrast, CJ THS positively respond to iTBZ. The colonization of the carbon felt even increased as the irradiation dose of the iTBZ was intensified. These findings may suggest that the gamma degradation products of TBZ inhibit the growth of microorganisms from the TSH SM, while on the contrary they promote the development of those from TSH CJ.

3.3 Analysis of TBZ degradation

3.3.1 UV-visible analysis

UV-visible spectroscopy was used to identify possible TBZ degradation through analysis of change in absorbance spectra between treated and untreated TBZ in synthetic FVPWW. As shown in Figure 4 the absorption range of a 50 ppm nTBZ solution extends to wavelengths above 320 nm, at room temperature (25 ± 0.1°C). The spectrum of nTBZ shows three absorption maxima (λ_{max}) in the bands from 218 to 221 nm, from 240 to 243 nm and from 296 to 302 nm corresponding to electronic transitions π–π* of aromatics rings of thiazole, imidazole and benzene (Chen et al., 2017; Jalali and Dorraji, 2017; Oliveira et al., 2020). Figure 3 reported also the evolution of the absorption spectrum of TBZ during irradiation (iTBZ-1.0 kGy; iTBZ-4.0 kGy) and bioelectrochemical (CJ-iTBZ-1.0 kGy, CJ-iTBZ-4.0 kGy) experiments. We observe no shift in the λ_{max} absorption of the solution upon irradiation

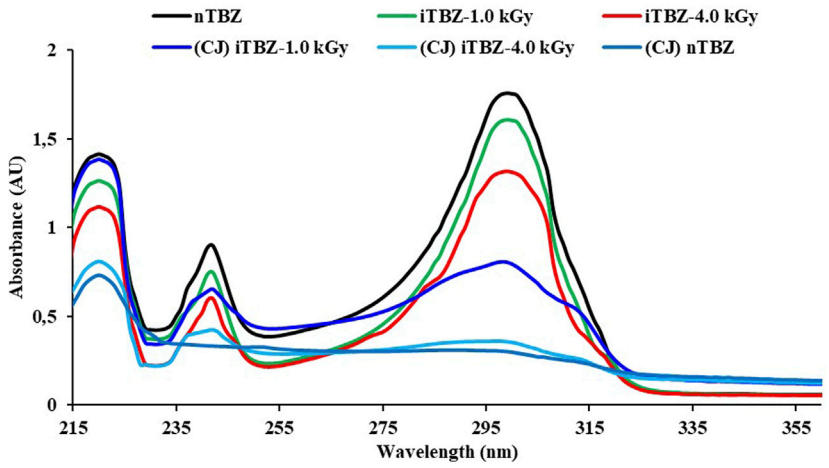

FIGURE 4
UV-visible spectrum of nTBZ, iTBZ-1.0 kGy and iTBZ-4.0 kGy before bioelectrochemical experiments and nTB, iTBZ-1.0 kGy and iTBZ-4.0 kGy after bioelectrochemical experiments with CJ as inoculums.

experiments (1 or 4 kGy), however there is a proportional decrease of the absorbance according to irradiation dose. It is worth noting that absorbance peaks at maximum wavelengths of nTBZ (λ_{max} 240 and 300 nm) were completely disappeared when nTBZ was treated by bioelectrochemical system containing CJ as source of halophilic bacteria. Furthermore, the disappearance of peaks at 240 and 300 nm argued in favor of total degradation of imidazole and benzene rings in nTBZ. The important decrease of the absorbance at 220 nm could demonstrate partial degradation of thiazole ring in nTBZ (Figure 3, CJ-nTBZ curve). By comparing CJ-nTBZ and CJ-iTBZ-4.0 kGy curves the degradation of TBZ is more effective without gamma irradiation pretreatment. In this case irradiation pretreatment does not improve TBZ degradation in the bioelectrochemical system. These findings strengthen the conclusions drawn from the COD removal and chronomaperometry analysis.

3.3.2 FTIR analysis

nTBZ, iTBZ and electrolytes from bioelectrochemical experiments were analyzed by FT-IR tool, between 400 and 4,000 cm^{-1}. FT-IR measurements were carried out to identify possible changes in nTBZ structure after irradiation and bioelectrochemical degradation. nTBZ consisted of benzimidazole and thiazole rings mainly composed of C–N, C=N, C=C, C–C, C–H, C–S and N–H groups. As shown in Figure 5 nTBZ absorption bands are confined from 3,100–430 cm^{-1} region, most of the peaks are displayed in the fingerprint region (1,500–400 cm^{-1}) demonstrate the complexity of the molecule. The FTIR spectrum of nTBZ revealed the presence of the C–H stretching of the benzene and the thiazole rings between 3,100 and 3,000 cm^{-1} (Silva et al., 2018). The bands around 2,980 cm^{-1} characterize tertiary amines C–N=C of the imidazole and the thiazole rings. Peaks at 1,623 and 1,403 cm^{-1} could be assigned to C=C stretch of both benzene and thiazole aromatics rings. Additionally, bands observed at 1,583 and 1,494 $cm^{-1}$are attributed to C=N and C–N stretching of the imidazole and the thiazole rings, respectively. The absorbance at 1,456 $cm^{-1}$is due to C=C–C of the aromatic rings (da Fonseca et al., 2015). The absorbance at 1,306 cm^{-1} could be associated to the C–N of imidazole and/or thiazole rings. Bands in the region between 1,012 and 985 cm^{-1} indicate C–S stretching of thiazole ring. The peaks observed between 1,278–1,096 $cm^{-1}$is due to C–C vibration and C–H in plane bend. However, absorbencies from 903 to 648 cm^{-1} are assigned to the out-of-plane bending vibration absorption peak of the benzene ring (Chen et al., 2021). As reported in Figure 5 considerable changes were observed in functional groups after TBZ degradation with both irradiation and bioelectrochimical techniques. More than twenty-five absorption peaks were observed before degradation of TBZ, while the number reduced to seven peaks after gamma irradiation and to five peaks after bioelectrochemical degradation of nTBZ. Moreover, the use of Gamma irradiation spanned peaks in the region of 1750 cm^{-1} to 680 cm^{-1}. Additionally, peaks were not the same between nTBZ and iTBZ, except for that observed at

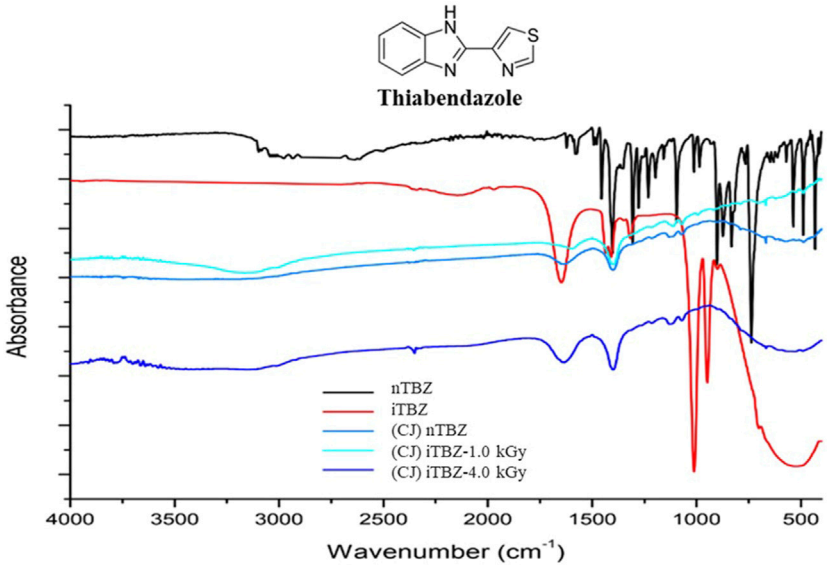

FIGURE 5
Fourier transform infrared (FT-IR) spectrum of nTBZ, iTBZ before bioelectrochemical experiments and nTBZ, iTBZ-1.0 kGy and iTBZ-4.0 kGy after bioelectrochemical experiments with CJ as inoculum.

1,012 cm^{-1} corresponded to C–S stretching of thiazole ring (Figure 5) which argued for partially degradation of thiol groups as explained above by UV-visible analysis. In fact, iTBZ FT-IR spectrum displayed new peaks at 1,650, 1,436, 1,411, 1,319 and 950 cm^{-1} which denoted the presence of C=C and N=C stretching and region between 700 and 400 cm^{-1} corresponding to C-H. These findings indicated that gamma irradiation impacted TBZ structure and leading to the formation of novel functional groups. After bioelectrochemical treatment of nTBZ, the thiol vibration peak of wave number at 1,012 and 985 cm^{-1} and CH bending were disappeared, indicating the breaking of the thiazole ring. Nonetheless, new functional groups had been shown in the spectra of CJ nTBZ confirming the degradation of TBZ and the formation of new metabolites. Compared with the FTIR spectrum of iTBZ bioelectrochemical degradation, no significant differences were observed. Several weak bands with low intensity were present after nTBZ bioelectrochemical degradation at 1,635–1,400, and 1,135–1,080 cm^{-1}. Thus, suggesting the complete degradation of TBZ using bioelectrochemical technique without the need of other prior procedure.

3.4 Bacterial analysis of the anodic biofilm

At the end of the operation period of the bioelectrochemical degradation of nTBZ using CJ as inoculum, biofilm samples on the anode surface and electrolyte were collected. Culture-dependent approach was applied to isolate bacterial strains community involved in TBZ degradation. As reported in Figure 6 at phylum level, the bacterial community was mainly presented by two phyla Proteobacteria (75%) and Firmicutes (25%). At species level *Bacillus velezensis*, *Bacillus spizizenii*, and *Bacillus inaquosorum* were isolated as Firmicutes strains. Then, *Halomonas smyrnensis*, *Halomonas halophila*, *Halomonas salina*, *Halomonas organivorans* and *Halomona skoreensis* as Proteobacteria strains.

Previous studies have shown the ability of these isolated strains to degrade several refractory toxic molecules (azo dyes, pesticides and hydrocarbons) and able to tolerate heavy metals. *B. velezensis* was reported as azo dye degrading bacterium (Bafana et al., 2008). Vörös et al. (2019) examined the ability of *B. velezensis* to tolerate heavy metals. It is also reported as pesticides degrading bacterium. Similarly, several study (Ishag et al., 2016; Ishag et al., 2017; Abdelbagi et al., 2018) reported the ability of *B. Inaquosorum* in the degradation of different

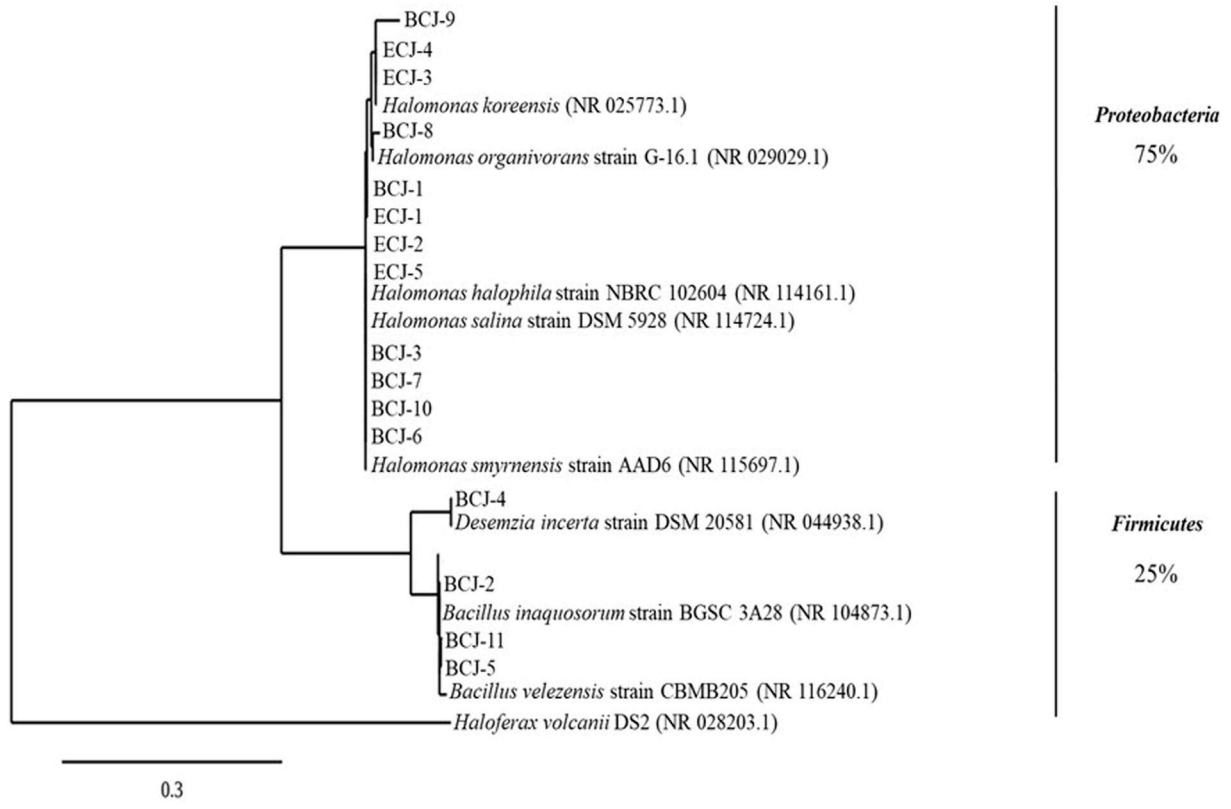

FIGURE 6
Phylogenetic tree of isolated species from biofilm and anolytes of nTBZ-CJ reactor by using culture depended approach. The taxonomy of the strains was determined *via* EzBioCloud. The phylogenetic dendrograms was constructed using the phylogeny. fr website.

pesticides such as chlorpyrifos, malathion, dimethoate, pendimethalin, endosulfan alpha and endosulfan beta. Moreover, *B. Inaquosorum*is shown to be involved in the treatment of recalcitrant petrochemicals (Ahmadi et al., 2019). *Halomonas* genus as well, has a considerable potential ability for degrading aromatic compounds of saline contaminated waters (CortiMonzón et al., 2018). It has been demonstrated that those isolates could degrade polycyclic aromatic hydrocarbons such as pyrene, fluoranthene, fluorine (Nanca et al., 2018; Govarthanan et al., 2020). In addition, *Halomonas sp*. are widely explored as dyes removal bacteria, they were used for decolorization of aqueous solution containing azo dyes such as Reactive Black 5 (RB5), Remazol Brilliant Violet 5 R (RV5), and Reactive Orange 16 (RO16) (Montañez-Barragán, et al., 2020). As these, strains have proven to be effective and live naturally in an environment highly contaminated by pesticides and have the potential to eliminate pesticides from contaminated waters, especially wastewaters from pesticide industries and landfill sites. Overall bacterial community structure at the genus level isolated from reactors containing TBZ was predominantly composed of *Halomonas* species (75%). These species were previously cited as electroactive bacteria and able to grow in high levels of salinity and possess particular electrochemical properties (Askri et al., 2019; Uma Maheswari et al., 2019; Liu and Wu, 2021).

4 Conclusion

This work demonstrated the potential to develop an efficient halotolerant bioanode incorporating bacteria from CJ THS. Under weak electrostimulation CJ THS halotolerant bacteria, composed mainly by *Halomonas* species, were able to rapidly degrade the recalcitrant fungicide TBZ in synthetic FPWW without gamma irradiation pretreatment. This study demonstrated that weak electrostimulation (3.66 mA/m^2) was necessary for enhancing the microbial transformation of nTBZ (50 ppm) and improved COD removal from 40 to 81%. THS halotolerant bacteria, specifically those from CJ site certainly have well established application for the electrostimulated microbial biodegradation of fungicide in the real fruit and vegetable processing industries. However, further studies will investigate the innocuity of the treated synthetic FPWW using suitable analytical tools, and clarify the roles of other bacterial members of the consortium using omic approaches.

Data availability statement

The original contributions presented in the study are included in the article/supplementary material, further inquiries can be directed to the corresponding authors.

Author contributions

NS, HC, BE, and AC: conceived and designed the experiments and analyzed the data. NS, HC, and SS: sampling. NS, BE, and HC: performed bioelectrochemical experiments. BE, NS, and HC: performed electrochemical analysis. AZ and HJ: performed gamma irradiation experiments. NS, HC, SS, and AC: performed microbial analyses. HC, NS, BE, AM, MN, RD, and AC: manuscript preparation and revision. HC, BE, and AC: supervised the entire project. All authors: contributed to the article and approved the submitted version.

Funding

This work was financially supported by the “PHC Utique” program of the French Ministry of Foreign Affairs and Ministry of higher education, research and innovation and the Tunisian Ministry of higher education and scientific research in the CMCU project number 20G1115.

Conflict of interest

The authors declare that the research was conducted in the absence of any commercial or financial relationships that could be construed as a potential conflict of interest.

Publisher’s note

References

Abdelbagi, A. O., Wady, A. I. A., Ishag, A. E. S. A., Hammad, A. M. A., Abdalla, M. A. O., and Hur, J. H. (2018). Biodegradation of fenthion and temphos in liqud media by Bacillus safensis isolated from pesticides polluted soil in the Sudan. *Afr. J. Biotechnol.* 17 (12), 396–404. doi:10.5897/AJB2017.16255

Ahmadi, M., Ahmadmoazzam, M., Saeedi, R., Abtahi, M., Ghafari, S., and Jorfi, S. (2019). Biological treatment of a saline and recalcitrant petrochemical wastewater by using a newly isolated halo-tolerant bacterial consortium in MBBR. *Desalination Water Treat* 167, 84–95. doi:10.5004/dwt.2019.24627

Ailijiang, N., Chang, J., Liang, P., Li, P., Wu, Q., Zhang, X., et al. (2016). Electrical stimulation on biodegradation of phenol and responses of microbial communities in conductive carriers supported biofilms of the bioelectrochemical reactor. *Bioresour. Technol.* 201, 1–7. doi:10.1016/j.biortech.2015.11.026

Askri, R., Erable, B., Etcheverry, L., Saadaoui, S., Neifar, M., Cherif, A., et al. (2020). Allochthonous and autochthonous halothermotolerant bioanodes from hypersaline sediment and textile wastewater: A promising microbial electrochemical process for energy recovery coupled with real textile wastewater treatment. *Front. Bioeng. Biotechnol.* 8, 609446. doi:10.3389/fbioe.2020.609446

Askri, R., Erable, B., Neifar, M., Etchevery, L., Masmoudi, A. S., Cherif, A., et al. (2019). Understanding the cumulative effects of salinity, temperature and inoculation size for the design of optimal halothermotolerant bioanodes from hypersaline sediments. *Bioelectrochemistry* 129, 179–188. doi:10.1016/j.bioelechem.2019.05.015

Bafana, A., Chakrabarti, T., and Devi, S. S. (2008). Azoreductase and dye detoxification activities of Bacillus velezensis strain AB. *Appl. Microbiol. Biotechnol.* 77, 1139–1144. doi:10.1007/s00253-007-1212-5

Baranitharan, E., Khan, M. R., Prasad, D. M. R., Teo, W. F. A., Tan, G. Y. A., and Jose, R. (2015). Effect of biofilm formation on the performance of microbial fuel cell for the treatment of palm oil mill effluent. *Bioprocess Biosyst. Eng.* 38 (1), 15–24. doi:10.1007/s00449-014-1239-9

Ben Abdallah, M., Karray, F., Kallel, N., Armougom, F., Mhiri, N., Quemeneur, M., et al. (2018). Abundance and diversity of prokaryotes in ephemeral hypersaline lake Chott El Jerid using Illumina Miseq sequencing, DGGE and qPCR assays. *Extremophiles* 22, 811–823. doi:10.1007/s00792-018-1040-9

Carra, I., Sirtori, C., Ponce-Robles, L., Pérez, J. A. S., Malato, S., and Agüera, A. (2015). Degradation and monitoring of acetamiprid, thiabendazole and their transformation products in an agro-food industry effluent during solar photo-Fenton treatment in a raceway pond reactor. *Chemosphere* 130, 73–81. doi:10.1016/j.chemosphere.2015.03.001

Castillo, L. E., Ruepert, C., and Solis, E. (2000). Pesticide residues in the aquatic environment of banana plantation areas in the north Atlantic zone of Costa Rica. *Environ. Toxicol. Chem.* 19, 1942–1950. doi:10.1002/etc.5620190802

Chandrakant, R. H., Ananda, J. J., Dipak, V. P., Naresh, M. M., and andAniruddha, B. (2016). A critical review on textile wastewater treatments: Possible approaches. *J. Environ. Manage.* 182, 351–366. doi:10.1016/j.jenvman.2016.07.090

Chen, G., An, X., Li, H., Lai, F., Yuan, E., Xia, X., et al. (2021). Detoxification of azo dye Direct Black G by thermophilic Anoxybacillus sp. PDR2 and its application potential in bioremediation. *Ecotoxicol. Environ. Saf.* 214, 112084. doi:10.1016/j.ecoenv.2021.112084

Chen, Q., Zuo, J., He, X., Mo, X., Tong, P., and Zhang, L. (2017). Enhanced fluorescence of terbium with thiabendazole and application in determining trace amounts of terbium and thiabendazole. *Talanta* 162, 540–546. doi:10.1016/j.talanta.2016.10.036

Cherif, H., Neifar, M., Chouchane, H., Soussi, A., Hamdi, C., Guesmi, A., et al. (2017). "Extremophile diversity and biotechnological potential from desert environments and saline systems of southern Tunisia," in *Extremophiles: From biology to Biotechnology*. Editors V. Ravi, D. Durvasula, and V. Subba Rao (Boca Raton, FL: CRC Publishers), 33–64.

CortiMonzón, G., Nisenbaum, M., Herrera Seitz, K., and Murialdo, S. E. (2018). New findings on aromatic compounds degradation and their metabolic pathways, the biosurfactant production and motility of the halophilic bacterium *Halomonas* sp. *KHS3. Curr. Microbiol.* 75, 1108–1118. doi:10.1007/s00284-018-1497-x

da Fonseca, R. J., Segatelli, M. G., Borges, K. B., and Tarley, C. R. T. (2015). Synthesis and evaluation of different adsorbents based on poly (methacrylic acid–trimethylolpropane trimethacrylate) and poly (vinylimidazole–trimethylolpropane trimethacrylate) for the adsorption of tebuthiuron from aqueous medium. *React. Funct. Polym.* 93, 1–9. doi:10.1016/j.reactfunctpolym.2015.05.004

Elabed, A., El khalfaouy, R., Ibnsouda, S., Basseguy, R., Elabed, S., and Erable, B. (2019). Low-cost electrode modification to upgrade the bioelectrocatalytic oxidation of tannery wastewater using acclimated activated sludge. *Appl. Sci. (Basel).* 9, 2259. doi:10.3390/app9112259

Ettoumi, B., Guesmi, A., Brusetti, L., Borin, S., Najjari, A., Boudabous, A., et al. (2013). Microdiversity of deep-sea Bacillales isolated from Tyrrhenian Sea sediments as revealed by ARISA, 16S rRNA gene sequencing and BOX-PCR fingerprinting. *Microbes Environ.* 28, 361–369. doi:10.1264/jsme2.ME13013

European Commission (Ec) (2013). Draft renewal assessment report prepared according to the Commission Regulation (EU) N.1141/2010. Report.

European Commission (Ec) (2001). Review report for the active substance thiabendazole finalised in the Standing Committee on Plant Health at its meeting on 12 December 2000 in view of the inclusion of thiabendazole in Annex I of Directive 91/414/EEC. 7603/VI/97-final.

Feng, H., Zhang, X., Guo, K., Vaiopoulou, E., Shen, D., Long, Y., et al. (2015). Electrical stimulation improves microbial salinity resistance and organofluorine removal in bioelectrochemical systems. *Appl. Environ. Microbiol.* 81 (11), 3737–3744. doi:10.1128/AEM.04066-14

Govarthanan, M., Khalifa, A. Y., Kamala-Kannan, S., Srinivasan, P., Selvankumar, T., Selvam, K., et al. (2020). Significance of allochthonous brackish water Halomonas sp. on biodegradation of low and high molecular weight polycyclic aromatic hydrocarbons. *Chemosphere* 243, 125389. doi:10.1016/j.chemosphere.2019.125389

Grattieri, M., and Minteer, S. D. (2018). Microbial fuel cells in saline and hypersaline environments: Advancements, challenges and future perspectives. *Bioelectrochemistry* 120, 127–137. doi:10.1016/j.bioelechem.2017.12.004

Ishag, A. E. S. A., Abdelbagi, A. O., Hammad, A. M. A., Elsheikh, E. A. E., Elsaid, O. E., Hur, J. H., et al. (2016). Biodegradation of chlorpyrifos, malathion, and dimethoate by three strains of bacteria isolated from pesticide-polluted soils in Sudan. *J. Agric. Food Chem.* 64, 8491–8498. doi:10.1021/acs.jafc.6b03334

Ishag, A. E. S. A., Abdelbagi, A. O., Hammad, A. M. A., Elsheikh, E. A. E., Elsaid, O. E., and Hur, J. H. (2017). Biodegradation of endosulfan and pendimethalin by three strains of bacteria isolated from pesticides-polluted soils in the Sudan. *Appl. Biol. Chem.* 60, 287–297. doi:10.1007/s13765-017-0281-0

Jalali, F., and Dorraji, P. S. (2017). Interaction of anthelmintic drug (thiabendazole) with DNA: Spectroscopic and molecular modeling studies. *Arabian J. Chem.* 10, S3947–S3954. doi:10.1016/j.arabjc.2014.06.001

Jiang, M., Ye, K., Deng, J., Lin, J., Ye, W., Zhao, S., et al. (2018). Conventional ultrafiltration as effective strategy for dye/salt fractionation in textile wastewater treatment. *Environ. Sci. Technol.* 52, 10698e10708–10708. doi:10.1021/acs.est.8b02984

Jiménez, M., Maldonado, M. I., Rodríguez, E. M., Ramírez, H. A., Saggioro, E., Carra, I., et al. (2015). Supported TiO_2 solar photocatalysis at semi-pilot scale: Degradation of pesticides found in citrus processing industry wastewater, reactivity and influence of photogeneratedspecies. *J. Chem. Technol. Biotechnol.* 90, 149–157. doi:10.1002/jctb.4299

Karuppiah, T., Pugazhendi, A., Subramanian, S., Jamal, M. T., and Jeyakumar, R. B. (2018). Deriving electricity from dye processing wastewater using single chamber microbial fuel cell with carbon brush anode and platinum nano coated air cathode. *3 Biotech.* 8 (10), 437–439. doi:10.1007/s13205-018-1462-1

Li, W.-J., Xu, P., Schumann, P., Zhang, Y.-Q., Pukall, R., Xu, L.-H., et al. (2007). Georgeniaruanii sp. nov., a novel actinobacterium isolated from forest soil in Yunnan (China), and emended description of the genus Georgenia. *Int. J. Syst. Evol. Microbiol.* 57, 1424–1428. doi:10.1099/ijs.0.64749-0

Liang, Y., Zhai, H., Liu, B., Ji, M., and Li, J. (2020). Carbon nanomaterial-modified graphite felt as an anode enhanced the power production and polycyclic aromatic hydrocarbon removal in sediment microbial fuel cells. *Sci. Total Environ.* 713, 136483. doi:10.1016/j.scitotenv.2019.136483

Liu, W., and Wu, Y. (2021). Simultaneous nitrification, denitrification and electricity recovery of Halomonas strains in single chamber microbial fuel cells for seawater sewage treatment. *J. Environ. Chem. Eng.* 9 (6), 106761. doi:10.1016/j.jece.2021.106761

Masiá, A., Campo, J., Vázquez-Roig, P., Blasco, C., and Picó, Y. (2013). Screening of currently used pesticides in water, sediments and biota of the Guadalquivir River Basin (Spain). *J. Hazard. Mat.* 263, 95–104. doi:10.1016/j.jhazmat.2013.09.035

M'Garrech, S., Jelassi, H., Mejri, A., and Ayadi, N. (2012). An empirical model for predicting the color variation of biologic molecules as a function of irradiation dose. *J. Radioanal. Nucl. Chem.* 295, 67–75. doi:10.1007/s10967-012-1847-2

Mohanakrishna, G., Al-Raoush, R. I., Abu-Reesh, I. M., and Pant, D. (2019). A microbial fuel cell configured for the remediation of recalcitrant pollutants in soil environment. *RSC Adv.* 9 (71), 41409–41418. doi:10.3389/fenrg.2021.672817

Montañez-Barragán, B., Sanz-Martín, J. L., Gutiérrez-Macías, P. P., Morato-Cerro, A., Rodríguez-Vázquez, R., and Barragán-Huerta, B. E. (2020). Azo dyes decolorization underhigh alkalinity and salinity conditions by Halomonas sp. in batch and packed bed reactor. *Extremophiles* 24, 239–247. doi:10.1007/s00792-019-01149-w

Nanca, C. L., Neri, K. D., Ngo, A. C. R., Bennett, R. M., and Dedeles, G. R. (2018). Degradation of polycyclic aromatic hydrocarbons by moderately halophilic bacteria from luzon salt beds. *J. Health Pollut.* 8, 180915–181010. doi:10.5696/2156-9614-8.19.180915

Oliveira, M. J., Rubira, R. J., Furini, L. N., Batagin-Neto, A., and Constantino, C. J. (2020). Detection of thiabendazole fungicide/parasiticide by SERS: Quantitative analysis and adsorption mechanism. *Appl. Surf. Sci.* 517, 145786. doi:10.1016/j.apsusc.2020.145786

Ounalli, L., Bhar, M., Mejri, A., Manai, K., Bouabidi, A., Abdallah, S. M., et al. (2017). Combining Monte Carlo simulations and dosimetry measurements for

process control in the Tunisian Cobalt-60 irradiator after three half lives of the source. *Nucl. Sci. Tech* 28, 133–144. doi:10.1007/s41365-017-0289-5

Papadopoulou, E. S., Genitsaris, S., Omirou, M., Perruchon, C., Stamatopoulou, A., Ioannides, I., et al. (2018). Bioaugmentation of thiabendazole-contaminated soils from a wastewater disposal site: Factors driving the efficacy of this strategy and the diversity of the indigenous soil bacterial community. *Environ. Pollut.* 233, 16–25. doi:10.1016/j.envpol.2017.10.021

Peréz, J. S., Carra, I., Sirtori, C., Agüera, A., and Esteban, B. (2014). Fate of thiabendazole through the treatment of a simulated agro-food industrial effluent by combined MBR/Fenton processes at μg/L scale. *Water Res.* 51, 55–63. doi:10.1016/j.watres.2013.07.039

Perruchon, C., Chatzinotas, A., Omirou, M., Vasileiadis, S., Menkissoglou-Spiroudi, U., and Karpouzas, D. G. (2017). Isolation of a bacterial consortium able to degrade the fungicide thiabendazole: The key role of a sphingomonas phylotype. *Appl. Microbiol. Biotechnol.* 101, 3881–3893. doi:10.1007/s00253-017-8128-5

Portillo, M. G., Aviño, E. S., Vicente, J. O., De Andrés, R. L., Jiménez, M. D. L. A. S., Blanco, J. P. L., et al. (2004). *Purification system for wastewater coming from fruit and vegetable processing plants and phytosanitary treatments in the field*. U.S. Patent No. 6,709,585. Washington, DC: U.S. Patent and Trademark Office.

Priyadarshini, M., Das, I., Ghangrekar, M. M., and Blaney, L. (2022). Advanced oxidation processes: Performance, advantages, and scale-up of emerging technologies. *J. Environ. Manage.* 316, 115295. doi:10.1016/j.jenvman.2022.115295

Pugazhendi, A., Al-Mutairi, A. E., Jamal, M. T., Jeyakumar, R. B., and Palanisamy, K. (2020). Treatment of seafood industrial wastewater coupled with electricity production using air cathode microbial fuel cell under saline condition. *Int. J. Energy Res.* 44 (15), 12535–12545. doi:10.1002/er.5774

Qian, X., Peng, X. H., Ansari, D. O., Yin-Goen, Q., Chen, G. Z., Shin, D. M., et al. (2008). *In vivo* tumor targeting and spectroscopic detection with surface-enhanced Raman nanoparticle tags. *Nat. Biotechnol.* 26, 83–90. doi:10.1038/nbt1377

Rousseau, R., Santaella, C., Achouak, W., Godon, J. J., Bonnafous, A., Bergel, A., et al. (2014). Correlation of the electrochemical kinetics of high-salinity-tolerant bioanodes with the structure and microbial composition of the biofilm. *ChemElectroChem* 1, 1966–1975. doi:10.1002/celc.201402153

Silva, M. D. S., Gonring, K. L., Silva, R. C. S. D., Fonseca, M. C., Borges, M. M. C., Nunes, O. C., et al. (2018). Fourier transform infrared spectroscopy, thermogravimetricanalysis, scanning electron microscopy as supporting tools in quality control of antiparasitics. *Quim. Nova* 41, 258–267. doi:10.21577/0100-4042.20170168

Uma Maheswari, R., Mohanapriya, C., Vijay, P., Rajmohan, K. S., and Gopinath, M. (2019). Bioelectricity production and desalination of Halomonas sp.–the preliminary integrity approach. *Biofuels* 10 (3), 355–363. doi:10.1080/17597269.2016.1242687

Vijay, A., Arora, S., Gupta, S., and Chhabra, M. (2018). Halophilic starch degrading bacteria isolated from sambhar lake, India, as potential anode catalyst in microbial fuel cell: A promising process for saline water treatment. *Bioresour. Technol.* 256, 391–398. doi:10.1016/j.biortech.2018.02.044

Vörös, M., Manczinger, L., Kredics, L., Szekeres, A., Shine, K., Alharbi, N. S., et al. (2019). Influence of agro-environmental pollutants on a biocontrol strain of Bacillus velezensis. *Microbiologyopen* 8 (3), e00660. doi:10.1002/mbo3.660

Wang, Z., Liang, B., Hou, Y., Li, S., Xie, L., Peng, L., et al. (2022). Weak electrostimulation enhanced the microbial transformation of ibuprofen and naproxen. *Sci. Total Environ.* 835, 155522. doi:10.1016/j.scitotenv.2022.155522

Yoon, S. H., Ha, S. M., Kwon, S., Lim, J., Kim, Y., Seo, H., et al. (2017). Introducing EzBioCloud: A taxonomically united database of 16S rRNA gene sequences and whole-genome assemblies. *Int. J. Syst. Evol. Microbiol.* 67, 1613–1617. doi:10.1099/ijsem.0.001755